Amplified-spontaneous-emission power oscillation in a beam-wave interaction

A. Bakhtyari, J. E. Walsh,* and J. H. Brownell
Department of Physics and Astronomy, Dartmouth College, Hanover, New Hampshire 03755-3528
(Received 24 September 2001; revised manuscript received 11 February 2002; published 11 June 2002)

We present in this paper compelling evidence supporting the three-wave traveling-wave theory developed by Pierce fifty years ago. The transition in a Smith-Purcell free-electron laser from low, through moderate amplified spontaneous emission, to strong gain conditions was carefully controlled. Below threshold, the emitted far-infrared power exhibits oscillations with a cubic dependence on the electron beam current. Both characteristics are expected in a three-wave interaction yet, to date, have not been observed.

DOI: 10.1103/PhysRevE.65.066503 PACS number(s): 41.60.−m, 84.40.Fe, 07.57.Hm, 42.60.Da

Free-electron lasers (FELs) are able to produce coherent radiation in regions of the electromagnetic spectrum inaccessible to traditional bound-electron devices, notably the far-infrared and x-ray regions. For this reason, much effort has been dedicated to their development and many different designs have been realized. Lasers based on the Cerenkov and Smith-Purcell [1] effects, traveling-wave interaction, undulator and magnetic bremsstrahlung radiation, and cyclotron resonance have all been demonstrated. It has been shown that the stimulating interaction providing the gain in each case share the same relations between spontaneous and stimulated emission parameters [2]. Therefore, shedding light on any of these interactions informs the entire field.

In 1946, several groups, that of Pierce among them, discovered the traveling-wave interaction and created the traveling-wave tube (TWT) to utilize it. Shortly after, Pierce described the interaction as the mutual feedback between the two electron beam space-charge waves and the copropagating resonant cavity wave [3]. TWTs typically operate with dense beams and so the collective action of the electrons was incorporated. Pierce derived a cubic dispersion relation, implying one of the three-wave components should grow exponentially with a rate proportional to the cube root of the electron number density ($n_0^{1/3}$). He assumed the cold beam limit in which the relative electron velocity spread is much smaller than the growth over one wavelength. Walsh extended the traveling-wave analysis to include warm beams [4]. He concluded that the gain in this limit is proportional to n_0.

Interestingly, a recent paper by Kim *et al.* [9], identifies yet another mode of operation. When the beam is narrow enough to neglect transverse propagation effects within it, the cold beam gain varies as the square root of n_0. It is important to note that this mode produces no power oscillations because both growing and decaying waves share the same phase.

In many cases, laser gain is calculated in the single-particle limit where the presence of the electron beam is assumed not to influence the resonant mode and so the work done on each particle separately determines the net growth of the mode amplitude [5,6]. This limit applies to FEL oscillators in which the single pass gain is typically weak. The single-particle result exhibits nonexponential gain with similar dependence on operating parameters to the warm beam case, contrary to Pierce's collective result, though they have been shown to be limits of the same underlying mechanism [7,8].

The Pierce theory predicts behavior in the output power that can be classified into three regimes: weak, moderate, and strong. The total power is the square of the sum of three amplitudes, one of which grows while another is attenuated. In the weak regime, growth is compensated by attenuation and output power is proportional to the current, which characterizes spontaneous emission. With strong gain, the growing wave dominates and the power grows exponentially with gain. It is the moderate regime, commonly called amplified spontaneous emission (ASE), that exhibits distinct behavior. Due to a gain dependent phase, the three waves beat against each other, producing oscillation in power with increasing gain. The applicable theoretical model can be distinguished by shape of this oscillation.

To our knowledge, only one observation of interference in a traveling-wave system has been reported. Ristic *et al.* [10] probed the surface waves propagating along a beam filled plasma column. Only weak gain was achieved. By mapping the wave amplitude as a function of distance along the axis, they found fringes that they attribute to interference between two waves of different phase velocities, the growing space-charge wave and the forward traveling resonant wave. This result implies the coexistence of two waves but does not identify the means of generating the growth. An earlier experiment by Boyd *et al.* [11] produced a growing wave but no evidence of beating with another.

This paper describes an experiment with a Smith-Purcell based FEL (SP FEL). Previously, we reported that an electron beam, produced in a scanning electron microscope, passing over a diffraction grating achieved strong gain at terahertz frequencies [12]. Super linear power was observed above a distinct threshold current level. Intriguing ripples appeared sporadically in that data but not sufficiently pronounced or reproducible as to warrant comment. By expanding the beam radius, thereby reducing the gain, we have been able to investigate the subthreshold ASE regime systematically.

Traveling-wave gain develops in an SP FEL as follows. An electron beam emits an evanescent wakefield while moving parallel to the grating surface and transverse to the rul-

*Deceased.

ings. The conductive surface reflects the field back into the beam which, in turn, forces the beam to coalesce into a train of bunches. The field with wavelength commensurate to the bunch spacing grows with the degree of bunching. In addition to providing the feedback for this fundamental mode, the periodic boundary scatters the wave throughout an infinite set of spatial harmonic orders. Energy is coupled out as Smith-Purcell radiation through harmonic orders that fall within the lightcone.

Pierce described this process by combining the wave, continuity, and Newton equations into a quartic dispersion relation, representing two counterpropagating, resonant modes supported by the cavity and two space-charge waves carried on the beam. Significant energy transfer among these fields occurs only when their phase velocities match (the synchronism condition). In this case, the dispersion relation factors into a real, cubic equation with complex roots.

The synchronous wave is necessarily ''slow'' and so is evanescent away from the grating surface. Therefore, the energy flow is strictly along the grating surface and in the direction of the beam, defined as $\hat{\mathbf{z}}$. Assuming the growth is purely spatial and defining the normal direction $\hat{\mathbf{x}}$, the field amplitude can be written as

$$\mathbf{E}=\mathbf{E}_0 g(y)\exp[-qx+i(kz-\omega t)], \tag{1}$$

where the frequency ω is real, the z component of the wave vector is complex, and $g(y)$ is the resonant mode distribution in y direction. The coefficient q is the inverse evanescent length.

Near synchronism, the three roots of the dispersion relation are

$$(\omega/v-k_j)=\alpha\{1/\sqrt{3}+i,\ 1/\sqrt{3}-i,\ -2/\sqrt{3}\}. \tag{2}$$

Given a beam of current I and relative energy γ and velocity $\beta=v/c$, the gain per unit length is

$$\alpha=\frac{\sqrt{3}}{2\beta\gamma}\left(\frac{I}{I_{\mathrm{A}}}\frac{\omega h}{\xi v_{\mathrm{group}} A_{\mathrm{mode}}}\right)^{1/3}, \tag{3}$$

where $I_{\mathrm{A}}=mc^3/e=17\ kA$, A_{mode} and v_{group} are the mode group velocity and transverse area, h is the normalized overlap of the beam and mode profiles, and ξ the fraction of the mode energy density contained in the longitudinal field.

Detected power is proportional to the total intensity of the interacting waves. In the weak to moderate gain regimes, all three waves have comparable amplitudes and must be included. The fourth, counterpropagating wave is far off-resonant and not excited by the beam. The detected power can then be related to the spontaneous emission P_{sp} (in the absence of gain) by

$$P_{\mathrm{det}}\propto\frac{P_{\mathrm{sp}}}{\Delta z}\int_z^{z+\Delta z}dz\left|\sum_{j=1}^{3}A_j e^{(ik_j-\Gamma_j)z}\right|^2, \tag{4}$$

where Δz is the range accepted by the detector, and Γ_j and $A_j=A_j\exp(i\phi_j)$ are the loss and initial complex amplitude of the jth wave, respectively. The detected power will oscillate with current due to the difference in the real parts of k_j. Note that P_{sp} is linear in I and Δz as long as the beam profile remains constant.

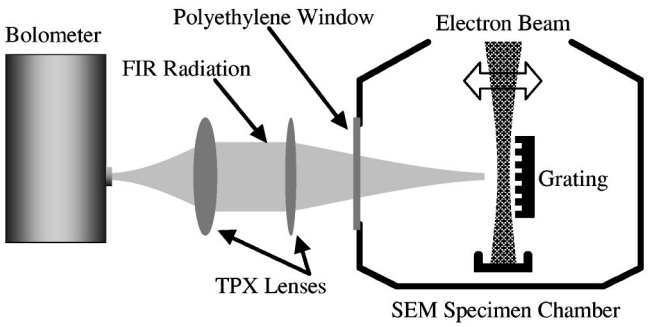

FIG. 1. Schematic of the experimental apparatus. The electron beam is swept over the face of the grating (in the direction indicated by the wide arrow) at 200 Hz. The center of the grating is imaged onto the active area of a helium cooled bolometer.

With nine independent parameters in Eq. (4), the gain cannot be determined with great certainty. In order to avoid this ambiguity, the threshold current I_{th} is defined to delineate the high gain region where the pure exponential term dominates. Given constant losses, initial phases, and beam profile, expanding the sum yields an expression that includes a pure exponential term and a growing amplitude sinusoidal term. Just below threshold the oscillating term dominates whereas above threshold the purely exponential term is responsible for the rapid rise in output power. At threshold, these terms are equal implying that the threshold gain is constant and equal to the loss on the growing mode.

The SP FEL consisted of a 1-cm-long diffraction grating, acting as a single element resonator, driven by a high quality electron beam produced with a modified scanning electron microscope (SEM). Figure 1 depicts the apparatus that is described in more detail in Ref. [12]. The grating employed in this experiment was aluminum alloy with rectangular profile of dimensions 180-μm period, 100-μm slot width, and 100-μm slot depth. The output was collected by a compound lens imaging the center of the grating onto the active area of a helium cooled Si-composite bolometer detector. Additional computer automation of the beam tuning and scanning functions allowed for tight control and real-time monitoring of the beam characteristics.

The beam profile was measured with a set of three vertically displaced, grounded wires mounted next to the grating on a translating table. The wires were placed to coincide with the center and either end of the grating. As the beam sweeps across each wire it casts a shadow, which is reflected in the signal from the Faraday cup collecting the beam after the grating. Given the wire diameter, the rise time of this signal indicates the beamwidth at the level of the wire.

In order to test the Pierce theory, the radiant power was recorded as a function of beam current for several acceleration voltage values ranging from 23 kV to 35 kV. The power was measured with a lock-in amplifier while sweeping the beam normally past the grating surface (in the plane of the page in Fig. 1). By this method, the total current could be

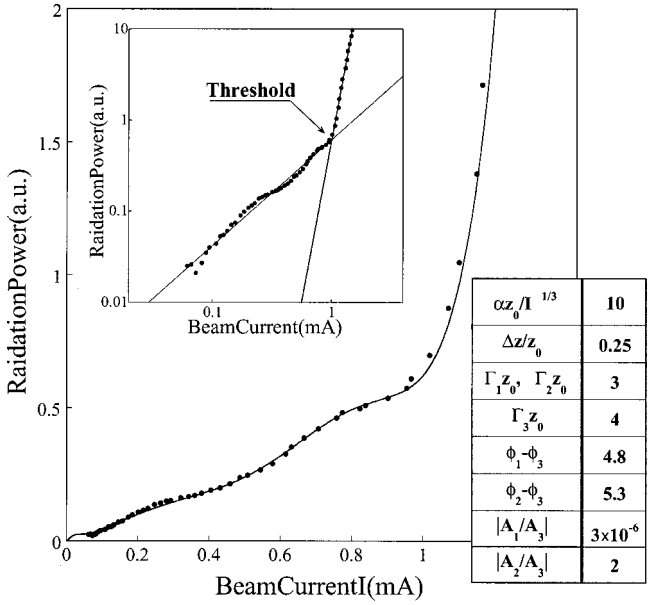

$\alpha z_0/I^{1/3}$	10
$\Delta z/z_0$	0.25
$\Gamma_1 z_0$, $\Gamma_2 z_0$	3
$\Gamma_3 z_0$	4
$\phi_1-\phi_3$	4.8
$\phi_2-\phi_3$	5.3
$\lvert A_1/A_3\rvert$	3×10^{-6}
$\lvert A_2/A_3\rvert$	2

FIG. 2. Plot of SP FEL radiant power vs electron beam current of a typical current scan. The solid line is a fit to Eq. (4). Inset: the same data plotted logarithmically. The threshold is defined to be the intersection of two power law fits to the regions above and below threshold.

recorded simultaneously. The SEM column was adjusted prior to each current scan to produce a beam profile of (60 ± 2) μm and (90 ± 8) μm full width at half maximum at the center and either end of the grating, respectively, (corresponding to a depth of field of roughly 5 mm). A separate measurement showed no discernible change in profile up to 1.2 mA. The tilt of the grating was adjusted to maximize the lock-in amplifier output, generally 1°–2° facing the beam. Also, the frequency of the output corresponding to first-order Smith-Purcell emission at 0.5 THz was verified by transmission grating filters.

Figure 2 shows a plot of radiant power vs current at 35 kV, which contains typical observed features. The power builds from a low level and then develops distinct oscillations up to a certain threshold above which monotonic rapid growth ensues. This indicates that the data spans the low, ASE, and high gain operating regimes. The solid line is the predicted power, Eq. (4), with the parameter values chosen to fit the data as indicated in the inset table. It is important to note that while the parameters were assumed constant for this fit, space-charge effects alter the beam profile and the resonant mode as the current is increased. The excellent agreement of the fit suggests that these effects are small.

It should be noted, however, that the fit parameters were found manually and some of them are certainly not unique. Changing the loss terms $(\Gamma_j z_0)$ by a factor of 2, with a commensurate change in the gain (α) results in a fit similar to the one shown in Fig. 2.

The disparate values for the losses Γ_i deserve further comment. Pierce investigated the effect of imposing a common loss into his theory and surmised that the initial amplitudes of the three waves should vary relatively with the degree of loss. This approach, in which the losses were set

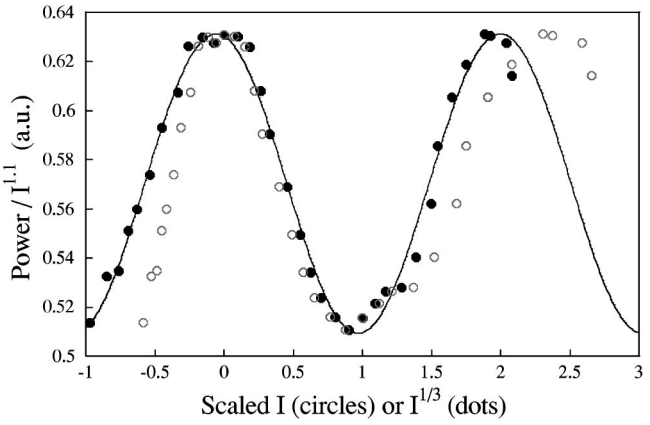

FIG. 3. A focus on the oscillating region. Dots represent the data plotted against $I^{1/3}$ along with the best sine curve fit. For comparison the same data set is plotted against I (circles), which cannot be fitted in the same way.

equal, resulted in a slightly inferior fit to that of Eq. (4). We present instead a generalization of Pierce's theory that produces the best fit to these data. It should be noted that our system is not strictly one dimensional. The influence of the electron transverse velocity spread and the asymmetric boundary conditions on the interaction is likely to be substantial and complex. The loss and phase parameters are aggregate indicators of these effects without suggesting a physical origin. The prominence of the power oscillations despite this complexity only fortifies the prediction that the three-wave interaction is the fundamental mode of operation.

The sinusoidal term in the expansion of Eq. (4) involves the growing and unattenuated waves (first and third). The second, attenuated wave has only weak influence in the ASE regime. Accordingly, the value of Γ_2 can be varied by more than an order of magnitude without diminishing the fit significantly. As noted above, Γ_1 determines the threshold while Γ_3 primarily affects the oscillation amplitude. Attributing different parameters to the individual waves is only justified if the modes are distinct. In the absence of loss, the modes are spaced by $\sqrt{3}\alpha$ with widths α, suggesting that they are just resolved. With loss, the modes are even more distinct because the net growth, and so the mode width, is smaller. In the Smith-Purcell case the loss originates primarily from coupling of power into the radiative mode.

The method employed for finding the threshold current is illustrated by the inset in Fig. 2, which is a logarithmic plot of the same data set. Subsets of the data (above and below threshold) were separately fitted to power law functions and the intersection of these lines determined I_{th}.

The subthreshold oscillations are clearly evident about the power law fit. When this section is plotted after normalizing by the fit (in this specific case the fit was $I^{1.1}$), the oscillation amplitude is constant. The three-wave model in the cold beam limit implies that the oscillations should be sinusiodal with $I^{1/3}$, while the warm beam limit implies the dependence is I. Figure 3 shows the subthreshold normalized power plotted twice, against $I^{1/3}$ (dots) and I (circles). For easier comparison the abscissae were scaled with the functions $(I-I_0)/(I_1-I_0)$ and $(I^{1/3}-I_0^{1/3})/(I_1^{1/3}-I_0^{1/3})$, respectively, to ensure that the first maximum (at I_0) and following mini-

mum (at I_1) coincide. The $I^{1/3}$ dependence is sinusoidal, as confirmed by the sine fit to the dots (solid line), while the period of the I dependence clearly increases with current. The conclusion that the SP FEL operates in the cold beam limit is reasonable considering that the thermionic cathode introduces only a few eV energy spread so that the relative velocity is only one percent of the growth per wavelength ($\Delta v/v \lesssim 0.01 \ \ \alpha/k$).

Together, the observation of oscillations with cubic dependence on current and the transition to exponential growth at high gain offer compelling evidence that the SP FEL operates in the cold beam limit through the three-wave interaction developed by Pierce. There are, however, three important implications from the theoretical fits. First, the growing wave must be initially smaller relative to the other two. If this were not the case, the growing wave would dominate long before an oscillation develops. Second, detecting only a narrow portion Δz of the grating is necessary for observing the oscillations. The fit suggests the detected power is emitted from a small fraction of the total interaction length, estimated to be between 5 and 10 mm. Varying the fitting parameter Δz reveals that the oscillations wash out when the viewed portion encompasses the full interaction length.

The authors would like to thank Professor William Doyle for valuable discussions. Support from ARO Grant Nos. DAAD19-99-0067, DAAG55-97-1-0230, and DAAD19-99-1-0024, NSF Grant No. ECS-0070491, and Vermont Photonics, Inc. is gratefully acknowledged.

[1] S.J. Smith and E.M. Purcell, Phys. Rev. **92**, 1069 (1953).
[2] A. Friedman, A. Gover, G. Kurizki, S. Ruschin, and A. Yariv, Rev. Mod. Phys. **60**, 471 (1988).
[3] J.R. Pierce, *Traveling-Wave Tubes* (D. Van Nostrand Company, New York, 1950).
[4] J. Walsh, in Quantum Electronics Conference and Free Electron Laser Workshop (Telluride, Colorado, 1977).
[5] W.B. Colson, Ph.D. thesis, California Institute of Technology, 1977.
[6] A. Yariv and C.C. Shih, Opt. Commun. **243**, 233 (1978).
[7] A. Gover and Z. Livni, Opt. Commun. **26**, 375 (1978).
[8] B. Johnson and J. Walsh, Phys. Rev. A **33**, 3199 (1986).
[9] K.-J. Kim and S.-B. Song, in Proceedings of the 22nd International FEL Conference 2001 (unpublished).
[10] V.M. Ristic, S.A. Self, and F.W. Crawford, J. Appl. Phys. **40**, 5244 (1969).
[11] G.D. Boyd, R.W. Gould, and L.M. Field, Proc. IRE **48**, 1906 (1961).
[12] J. Urata, M. Goldstein, M.F. Kimmitt, A. Naumov, C. Platt, and J.E. Walsh, Phys. Rev. Lett. **80**, 516 (1998).